Search for admixtures of massive neutrinos in the decay $\pi^+ \to \mu^+ + \nu$

M. Daum and P.-R. Kettle
SIN, Schweizerisches Institut für Nuklearforschung, CH-5234 Villigen, Switzerland

B. Jost*
SIN, Schweizerisches Institut für Nuklearforschung, CH-5234 Villigen, Switzerland
and IMP, Institut für Mittelenergiephysik der Eidgenössischen Technischen Hochschule, Zürich, c/o SIN, CH-5234 Villigen, Switzerland

R. M. Marshall, R. C. Minehart, W. A. Stephens, and K. O. H. Ziock
Physics Department, University of Virginia, Charlottesville, Virginia 22901
(Received 6 April 1987)

We have performed a search for admixtures of massive neutrinos in the pion decay $\pi^+ \to \mu^+ + \nu$ at the Swiss Institute for Nuclear Research (SIN). Positive pions were stopped in a high-purity germanium detector and the energy of their decay muons was measured with a resolution of 10 keV (full width at half maximum). The energy spectrum of the muons was searched for additional peaks, the existence of which would have indicated lepton mixing; no such peaks were found. The upper limit for the branching ratio for the decay of a pion into a muon and a heavy neutrino has been significantly improved for neutrino masses ranging from 1 to 16 MeV/c^2.

I. INTRODUCTION

In the minimal standard electroweak theory[1] all neutrinos are massless. This model, although extremely successful in predicting neutral weak currents and the masses of the intermediate vector bosons, has an asymmetry between neutrinos and the other fermions. One can introduce right-handed neutrinos in SU(2)⊗U(1); however, these are not required, in contrast with the other fields. Models based on a left-right-symmetric theory necessarily have right-handed neutrinos; they usually lead to a very heavy and a very light Majorana neutrino, or a massless and a relatively heavy Dirac neutrino.

If one considers the possibility of nonzero masses for neutrinos, for consistency one must also consider the leptonic mixing which in analogy to the quark mixing[2] would in general occur concomitantly.[3] This mixing can produce neutrino oscillations, a mechanism proposed to explain the solar-neutrino defect.[4] As pointed out by Shrock,[5] this mixing could also appear in weak decays. The weak eigenstates ν_l would consist of a mixture of mass eigenstates

$$\nu_l = \sum_i U_{l_i} \nu_i \ . \tag{1}$$

Here ν_i are the mass eigenstates and U_{l_i} the corresponding transformation matrix elements. Thus, if neutrinos are massive and nondegenerate then, for instance, the energy spectrum of the muons in the decay

$$\pi^+ \to \mu^+ + \nu \tag{2}$$

if kinematically allowed would consist of monochromatic lines at

$$T_i = (m_\pi{}^2 + m_\mu{}^2 - 2m_\pi m_\mu - m_{\nu_i}{}^2)/2m_\pi \ . \tag{3}$$

Here T_i is the kinetic energy of the muons, and m_π, m_μ, and m_{ν_i} are the masses of the pion, the muon, and the neutrino in the ith mass eigenstate, respectively. For a massless neutrino T_0 is 4120 keV; with the emission of a heavy neutrino the kinetic energy T_i of the muon would be lower. Thus one might expect to see additional peaks in the muon energy spectrum—one for each mass eigenstate of a massive neutrino—positioned below the peak at T_0 associated with zero (or a very small) neutrino mass.

Experimentally the decay of a pion into a muon and a heavy neutrino ν_i could be observed provided that (i) the mass of the neutrino m_{ν_i} is large enough in order that the muon energy could be distinguished from the main peak within the resolution of the detector system, (ii) m_{ν_i} is smaller than the mass difference between the pion and the muon (33.9 MeV/c^2), and (iii) the branching ratio is large enough to produce an observable peak.

Besides the decay (2) various experimental searches for heavy-neutrino states have been performed which generally complement each other both in sensitivity of U_{l_i} and in the mass range investigated. For a review we refer to Ref. 6. Up to now there has been no evidence for the number of generations in quark and lepton families being greater than three. The upper limit of m_{ν_τ}, the mass of the neutral lepton of the third generation, is 70 MeV/c^2 (Ref. 7) with a confidence level of 95%, and

therefore the kinematic range of the decay (2) ($0 \leq m_{\nu_i} \leq 33.9$ MeV/c^2) is of special interest for searches for admixtures of heavy neutrinos.

Experimental searches for heavy-neutrino states in pion decay have been performed using surface muon beams,[8] spectrometers,[8–10] or scintillation counters[11] in order to measure the muon energy spectrum. The use of surface muon beams as high-intensity spectrometers[8] is limited by the requirements for a high stability of the primary proton beam on the pion production target. While in spectrometer experiments[8–10] the resolution was very good, the counting rates achieved decrease strongly with increasing momentum resolution and thus limit the statistical significance of these searches. This problem was overcome by stopping pions in a plastic scintillator and measuring the height of the scintillation pulses associated with the subsequent decay muons.[11] The limited energy resolution of this method restricted this search to neutrino masses greater than 4 MeV/c^2.

In this experiment we have stopped positively charged pions in the center of a high-purity germanium detector, and measured the energy of the decay muons in the same detector using pulse sampling,[12] thereby combining the high energy resolution of solid-state detectors with a 4π acceptance solid angle for the decay muons. The difficulty with this method is that the rise time of a pulse from a germanium detector is of the same order as the pion lifetime. This forced us to discard most of our events, namely, all those in which the pion decayed during the rise of its pulse.

II. EXPERIMENTAL METHOD

A. The pion beam

Positive pions from the SIN pion channel πM3 (Ref. 13) were used. These pions are produced by 590-MeV protons from the ring accelerator in a 1-g/cm^2 carbon target under an angle of 22.5 deg. The solid-angle acceptance of the channel is 10 msr and the accepted momentum band is 8% [full width at half maximum (FWHM)]. The beam line was tuned to a momentum of 110 MeV/c with a 1.9% momentum spread. The large contamination of positrons in the beam line ($e^+/\pi^+ \simeq 3$) was suppressed by a 5-mm-thick graphite degrader placed at the intermediate focus of the beam.[14] For a momentum of 110 MeV/c this graphite degrader reduces the momentum of the pions by 3.5 MeV/c and the momentum of the positrons by 1.7 MeV/c; the angle of deflection in the following bending magnet then differs by 14 mrad and the separation of the two different particle type beams at the end of the beam line is 3.5 cm. In this way 90% of the positrons were blocked by a lead collimator. Further suppression was achieved by taking advantage of the different times of flight of positrons and pions of the same momentum in the beam line as well as the different energy losses in the detectors.

B. The experimental arrangement

Our experimental arrangement is shown in Fig. 1. Pions entered the apparatus and traversed a scintillation-counter telescope, $S1$ and $S2$. A 10-cm-thick lead collimator, with an aperture of 1-cm diameter was placed between $S1$ and $S2$ in order to block the beam positrons. The pions were slowed down by means of an aluminum degrader of variable thickness and entered the germanium detector telescope, composed of three detectors, through a 1-mm-thick aluminum window; they were stopped in the center of the germanium detector Ge2. The Ge detector telescope was surrounded by two scintillation counters $S3$ and $S4$, designed to intercept a large fraction of the positrons from the subsequent muon decays.

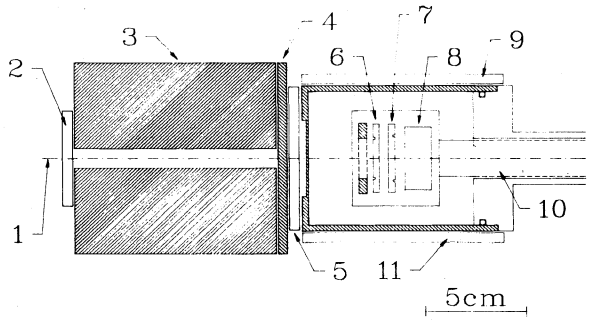

FIG. 1. Schematic diagram of the apparatus. (1) Axis of π^+ beam. (2) Scintillation counter $S1$. (3) Pion collimator and positron beam stopper (Pb). (4) Degrader (Al). (5) Scintillation counter $S2$. (6) Germanium detector Ge1. (7) Germanium detector Ge2 (pion stop detector). (8) Germanium detector Ge3. (9) Scintillation counter $S3$. (10) Cold finger. (11) Scintillation counter $S4$.

When a pion stopped in the detector Ge2 the output signal from its preamplifier had the general shape shown in Fig. 2: a superposition of the pulse heights from the stopping pion and the subsequent decay muon. The

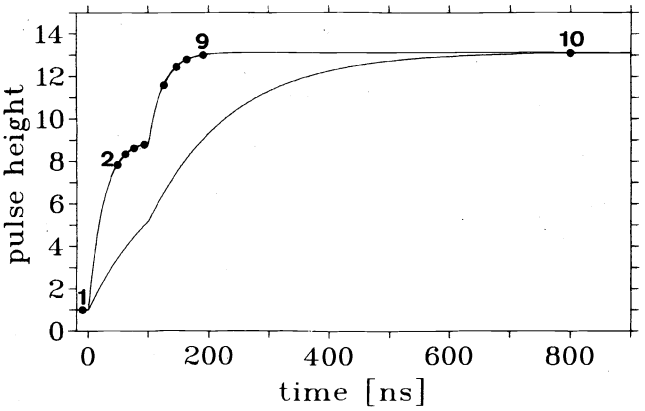

FIG. 2. Schematic pulse shape as seen by track and hold amplifiers. The ten sample points are marked by black dots. In this particular example, the pion decays 100 ns after its stop. The baseline is measured before the pion stop (sample point 1). The fast pulse is sampled eight times between 50 and 200 ns (sample points 2–9); the slow pulse is sampled once after 800 ns (sample point 10).

electronic rise time of the pulse was 25 ns. The aim of the experiment was to measure the muon pulses independently of the heights of the pion pulses. For this purpose the height of the signal was sampled at ten different points in time by multiplexing the signal to ten different track and hold (T&H) circuits. The first sampling point was taken prior to the arrival of the pion and served as a measure of the base line. Point 4 was chosen to define the height of the pion pulse and point 10 the sum of pion and muon energy. The other points were used to sample the shape of the pulse which provides information about the stopping depth of the pion in the detector, useful for cuts to be discussed later.

C. The germanium detectors

The germanium detectors were made for us by Dr. R. Pehl and his collaborators at the Lawrence Berkeley Laboratory. They consist of high-purity germanium. The *n* contacts were made by drifting lithium into a 0.1-mm layer of the detector; for the *p* contacts boron ions were implanted into a layer of thickness 0.2 μm. The detector Ge2 had an outer guard ring separated from the inner sensitive area by a groove in the *n* contact. This ring Ge2*R* was used as an anticounter to be described later.

The thicknesses of the detectors were 3.0, 3.4, and 13 mm; the diameters of their active areas were 20, 22.5, and 33 mm, respectively. The thickness of the detector Ge2 was chosen by consideration of the following constraints.

(a) The thickness of the detector has to be more than the range straggling of pions, stopped in the center of the detector Ge2. This range straggling is $\Delta R \simeq 0.5$ mm (rms) (Ref. 15).

(b) The range of muons from pion decay at rest is $R_\mu \simeq 0.4$ mm in germanium. This has to be added to the width obtained from range straggling both in the forward and backward direction.

(c) For optimal energy resolution the relative contribution of the stopping pion to the summed voltage of the pulses of the pion and the muon has to be small; thus the detector should be thin to minimize the contribution of the stopping pion.

(d) The time of charge collection should not be much larger than the mean lifetime of pions at rest so that the muon pulse is separated in time from the pion pulse in a sufficiently large part of the events.

The detector preamplifiers are described in Ref. 16. For the detector Ge2 a commercially available low-noise preamplifier (Tennelec TC170) was used to obtain maximum energy resolution.

D. The electronics

The data-aquisition system had to process signals from seven particle detectors; the electronic logics could thus be kept comparatively simple. For the timing of the coincidences the signals from the germanium detectors were fed through timing filter amplifiers (TFA's) and constant-fraction discriminators (CFD's). A pion stop in the detector Ge2 was indicated by the coincidence

$$\text{pion stop: } S1\cdot S2\cdot \text{Ge1}\cdot \text{Ge2}\cdot \text{RF}\cdot \overline{\text{Ge2}R}\cdot \overline{\text{Ge3}}\ .$$

Here RF is the radio frequency of the ring cyclotron (50 MHz), which is used for both the timing of the coincidence, and to distinguish pions from other beam particles by their time of flight in the pion channel. The energy deposited in the detector Ge2 is required to be consistent with the energy loss of a pion stopping within a central 1-mm-thick region. Almost all decay muons, the range of which is about 0.4 mm, should thus stop in the detector. The decay muons from such pion stops were only accepted within 75–200 ns after the pion stop signal, i.e., only 5.6% of all pion stops could be used. By accepting events with a shorter decay time t_π, where t_π is the time from the stop of a given pion to its decay, the energy resolution of our system would have been reduced considerably.[16,17] The decay muons were defined by the signature

$$\text{decay muon: } \text{Ge2}\cdot \overline{\text{Ge2}R}\cdot \overline{S1}\ .$$

Here the anticoincidence $\overline{S1}$ prevents beam particles from simulating a decay muon.

A combination of a pion stop signal with a decay muon event is a candidate for an accepted event. The decision whether the event will be accepted is made in a sequencer which also generates the ten hold signals for the (T&H) amplifiers and sends a signal to the PDP11/34 computer to start the readout of the data.

During the readout a fast software test is performed to ascertain that the candidate event is accompanied by a decay electron event with the logical signature

$$\text{decay electron: } \text{Ge2}\cdot(\text{Ge3}+S3+S4)\cdot\overline{\text{Ge1}}\cdot\overline{S1}$$

in the time interval ranging from 1 to 5 μs after the pion stop. Only events which contain the complete decay chain $\pi^+ \rightarrow \mu^+ \rightarrow e^+$ are written on tape. To ensure that only a single pion or muon was processed at any one time in the Ge detector telescope we rejected all events that were preceded or followed by another incident pion within about eight muon lifetimes (18 μs).

For the measurement of the pulse height in the pion stop detector Ge2 the pulses after amplification were fed into a (T&H) amplifier box consisting of ten (T&H) amplifiers. These amplifiers have an analog and a digital (logical) input. The output follows the analog input as long as the digital input is on logical 0; the amplifier is in the "track" mode. A change in the digital input from logical 0 to 1 results in a change of the output mode from "track" to "hold" after 8 ns. The output voltage is then constant. A change of the digital input from logical 1 to 0, switches to the "track" mode after about 100 ns.

At the first nine holding points (T&H) amplifiers THC-0300 (Analog Devices) with a bandwidth of 12 MHz were used. At holding point 10 a THC-1500 amplifier (Analog Devices) with a bandwidth of 1.2 MHz was used in order to obtain the highest precision for the measurement of the sum of the pion and muon energy. The time constants of these circuits were chosen to

match the requirements connected to the lifetimes of the pion and the muon.

(i) For the fast pulse the time constant of the electronics should be smaller than the pion lifetime or the time of charge collection in the detector Ge2 ($\simeq 25$ ns), so that the overall time constant of the fast pulse is not affected.

(ii) For the slow pulse the time constant should be large to obtain the desired energy resolution; however, it has to be small compared to the mean lifetime of the muon, since our trigger logics requires that the $(\pi+\mu)$ pulse height is measured before the decay of the muon.

The outputs of the (T&H) amplifiers were connected to the inputs of analog-to-digital converters (ADC's) with a resolution of 14 bit each. Here the voltage at the input had to be constant during the conversion time (12 μs). A more detailed description of the electronics is given in Ref. 16.

The event rates of our experiment at a primary proton beam intensity of 150 μA are presented in Table I. The rate of stopping pions had to match mainly the pile up probability originating from the long decay constant of the pulse (220 μs). At the pion beam line used for data taking a higher stopping rate could have been achieved by the selection of higher beam momentum and of a larger momentum spread; however, this would have lead to a larger width of the pion stopping distribution in the detector Ge2.

III. THE DATA ANALYSIS

A. Muon energy determination from pulse sampling

To explain the principle of the muon energy determination in a germanium detector the pulse shape is assumed in the following to be independent of the pulse height. Let the measured voltage for the time $t>0$ be

$$V(t)=V_0 f(t) \quad \text{for ADC's } 1-9 , \tag{4}$$

$$V(t)=V_0 g(t) \quad \text{for ADC } 10 , \tag{5}$$

$$V(t)=0 \quad \text{for } t<0 . \tag{6}$$

for $t<1$ μs the functions $f(t)$ and $g(t)$ are defined by the preamplifiers and (T&H) circuits, and increase with time constants of 25 and 135 ns, respectively. After reaching the plateau value at $t \lesssim 150$ ns for $f(t)$ and $t \simeq 800$ ns for $g(t)$, respectively, they decrease with e^{-t/τ_B}, where $\tau_B \simeq 220$ μs. The voltage V_0 is proportional to the energy deposited in the detector. For the sampling points $2 \le i \le 9$ the measured pulse height in the ADC is

$$A_i = V_\pi f(t_i) + V_\mu f(t_i - t_\pi) + A_1 e^{-(t_i - t_1)/\tau_B} . \tag{7}$$

Here t_i is the time of holding point i (cf. Fig. 2), t_π is the decay time of the pion, V_π and V_μ are voltages proportional to the energy of the pion and the muon, respectively, and A_1 is the height of the baseline. For $t_\pi > t_i$ one can see from Eqs. (6) and (7) that A_i is proportional to the pion energy alone:

$$A_i = V_\pi f(t_i) + A_1 e^{-(t_i - t_1)/\tau_B} . \tag{8}$$

For accepted events t_{10} is always larger than t_π and hence

$$A_{10} = V_\pi g(t_{10}) + V_\mu g(t_{10} - t_\pi) + A_1 e^{-(t_{10} - t_1)/\tau_B} . \tag{9}$$

With this one can determine the energy of the muon

$$V_\mu = \alpha_{10}(A_{10} - A_1) - \alpha_i (A_i - A_1) + \beta_i A_1 , \tag{10}$$

where

$$\alpha_{10} = 1/g(t_{10} - t_\pi) , \tag{11}$$

$$\alpha_i = \alpha_{10} g(t_{10})/f(t_i) , \tag{12}$$

$$\beta_i = (1 - e^{-(t_{10} - t_1)/\tau_B})\alpha_{10} - (1 - e^{-(t_i - t_1)/\tau_B})\alpha_i . \tag{13}$$

From Eq. (10) one can see that the difference $(A_{10} - A_i)$ is a linear function of $(A_i - A_1)$. The experimental distributions of $(A_{10} - A_i)$ against $(A_4 - A_1)$, i.e., the muon pulse heights against the pion pulse heights, are shown in Figs. 3 and 4 for $i=2$ and 4. The deviation from a straight line is clearly visible; it is the larger the earlier the pion energy is measured, and thus indicates a change of the pulse shape with the pulse height in contradiction to the assumption made above. This effect originates from the charge collection in the detector which is not fast compared to the typical time of in-

TABLE I. Typical event rates for a proton beam intensity of 150 μA. The decay e^+ rate is higher than the decay μ^+ rate because we accept muons from $75 \le t_\pi \le 200$ ns after the pion stop, while positrons are accepted for muon decay times $1 \le t_\mu \le 5$ μs. The solid-angle acceptance for positrons is smaller than that for muons (see Fig. 1).

Type of event	Rate (s^{-1})
π^+ stop	580
Decay μ^+	50
Decay e^+	164
Accepted events	10

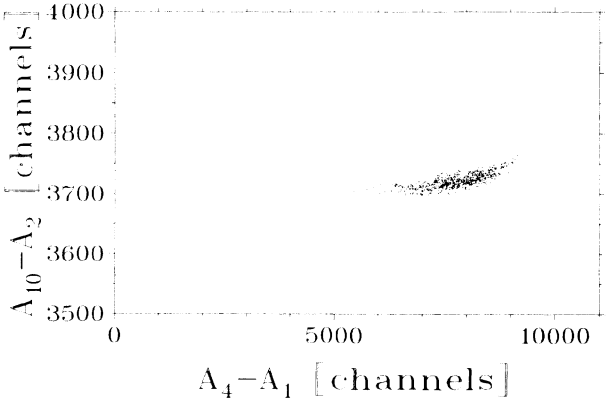

FIG. 3. Two-dimensional scatter plot of the muon energy from the sample points 10 and 2 (vertical axis) vs the pion energy from sample points 4 and 1 (horizontal axis).

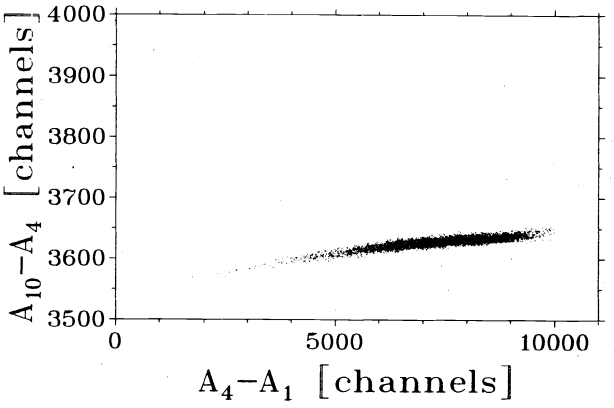

FIG. 4. Two-dimensional scatter plot of the muon energy from the sample points 10 and 4 (vertical axis) vs the pion energy from sample points 4 and 1 (horizontal axis).

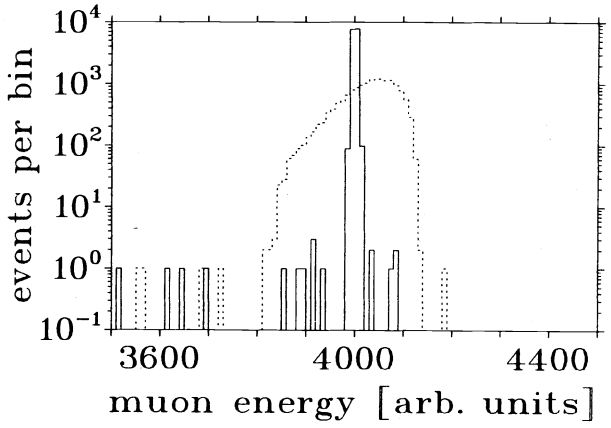

FIG. 5. Muon energy distribution before (dashed line) and after the correction. The two curves represent the same set of events.

tegration of the associated amplifiers. In addition the charge collection is coupled to the position of formation of the charge cloud in the detector, i.e., the particle track in the detector Ge2 (cf. Ref. 16). Thus the pulse height of a pion at a time $(t_i - t_1)$, i.e., its pulse shape, depends on the trajectory of the pion in the detector, and is a function mainly of its energy (see also Ref. 18).

This dependence of the pulse shape on the trajectory in the detector obviously complicates the analysis of the data. On the other hand, one can use this fact to reduce the background: pions which have been scattered backwards and stop near the upstream face of the detector can contribute to the background if their decay muons escape from the detector before stopping. Part of these pions can be distinguished by their pulse shape from those of the same energy stopping in the center of the detector Ge2 (see Sec. III C).

B. The correction of the muon energy

Projecting the data of Figs. 3 and 4 onto the ordinate results in a broad peak in the muon energy spectrum. By applying to the muon pulse height a correction depending on the details of the event (pion energy, pion decay time) the width of this peak can be significantly improved.

We have corrected the muon energy by means of a polynomial function, the coefficients of which were determined from the experimental data. For the energy ϵ_μ of the muons we have assumed

$$\epsilon_\mu^k = A_{10}^k - A_4^k - \mathcal{P}(A_4^k - A_1^k) - \mathcal{Q}(A_1^k) - \mathcal{R}(t_\pi^k) \ . \quad (14)$$

Here $t_\pi > t_4$, k is the event number and $\mathcal{P}$, $\mathcal{Q}$, and $\mathcal{R}$ are the polynomials which are independent of the event number and valid for a complete run. To find the polynomials we divided the abscissa (Figs. 3 and 4) into 100 bins and determined the mean values ϵ_μ for each bin. Using these mean values we calculated the polynomial coefficients by minimization of χ^2. The muon energy of each event was then corrected with these coefficients. The result is displayed in Fig. 5; the two curves in this figure represent the identical set of events, before and after the correction.

A further reduction of the width of the muon energy peak was obtained for each run by adjusting the energy scale slightly to center the peak of the muons from the two-body decay (2) at 4120 keV. The adjustment factors differed from unity by typically 0.1%; their variation is attributed to electronic drifts.

C. The reduction of the background

It is expected that some muons will leak out of the germanium detector Ge2 into the annular region Ge2R, which serves as a guard ring (cf. Sec. II C). Any muons making measurable pulses in the guard ring are discarded. However, some muons can escape from the central region and stop in the small dead region between the central and the annular outer region and thus are not registered in the guard ring. They are indistinguishable

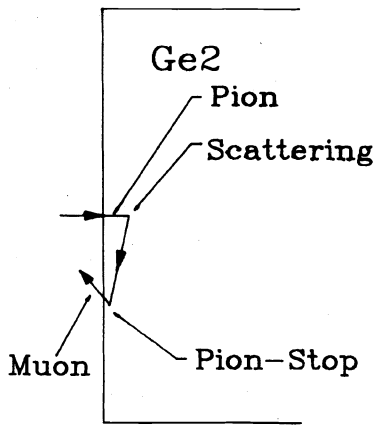

FIG. 6. Schematic diagram of a possible background event: a pion enters the pion stop detector Ge2 and is scattered backwards. The decay muon can leave the detector thereby depositing only part of its energy in the detector Ge2.

from the signal produced by the decay into a heavy neutrino and cause a continuous background.

Another contribution to the background originates from pions that were scattered backwards in the detector Ge2 and stop near the entrance face after having deposited an amount of energy consistent with having stopped in the center of the detector (see Fig. 6). Their associated decay muons can leave the front surface of the detector thereby depositing only part of their energy in the detector Ge2. Most of this background can be rejected by analyzing the shape of the pion pulse in the detector Ge2.

As can be shown by a Monte Carlo calculation most of the pions incident on the detector Ge2 stop in the center of the detector. These pions define a nominal pulse shape, which we describe by the following variables x_i:

$$\begin{aligned} x_1 &= A_4 - A_2 \ , \\ x_2 &= A_4 - A_3 \ , \\ x_3 &= (A_2 - A_1)/(A_4 - A_1) \ , \\ x_4 &= (A_3 - A_1)/(A_4 - A_1) \ , \end{aligned} \tag{15}$$

and combinations of these. The distributions of the x_i's are displayed in Fig. 7. A Gaussian has been fitted to these distributions using the computer program MINUIT (Ref. 19) to determine the mean value μ_i and the standard deviation σ_i of the variables x_i. With this a χ^2 can be calculated for each event

$$\chi^2 = \sum_{i=1}^{n} (x_i - \mu_i)^2 / \sigma_i^2 \ . \tag{16}$$

The χ^2 distribution of the events of one run is shown in Fig. 8. The events in the peak are represented by the continuous line, and the events outside the peak region by the dashed histogram. Limiting the allowed χ^2 value for each event to $\chi^2 \leq 10$ (for 7 degrees of freedom) reduces the number of events in the peak by 25% and the number of events outside the peak by 50%. It should be noted that these cuts do not affect the detection of a decay into a heavy neutrino because they are applied only to that part of the pulse originating from the incident pion. The relative merit of this method was verified by a Monte Carlo calculation.

IV. RESULTS AND DISCUSSION

A. The muon spectrum

The final muon energy spectrum after the cuts is shown in Fig. 9. One can see a narrow peak with a

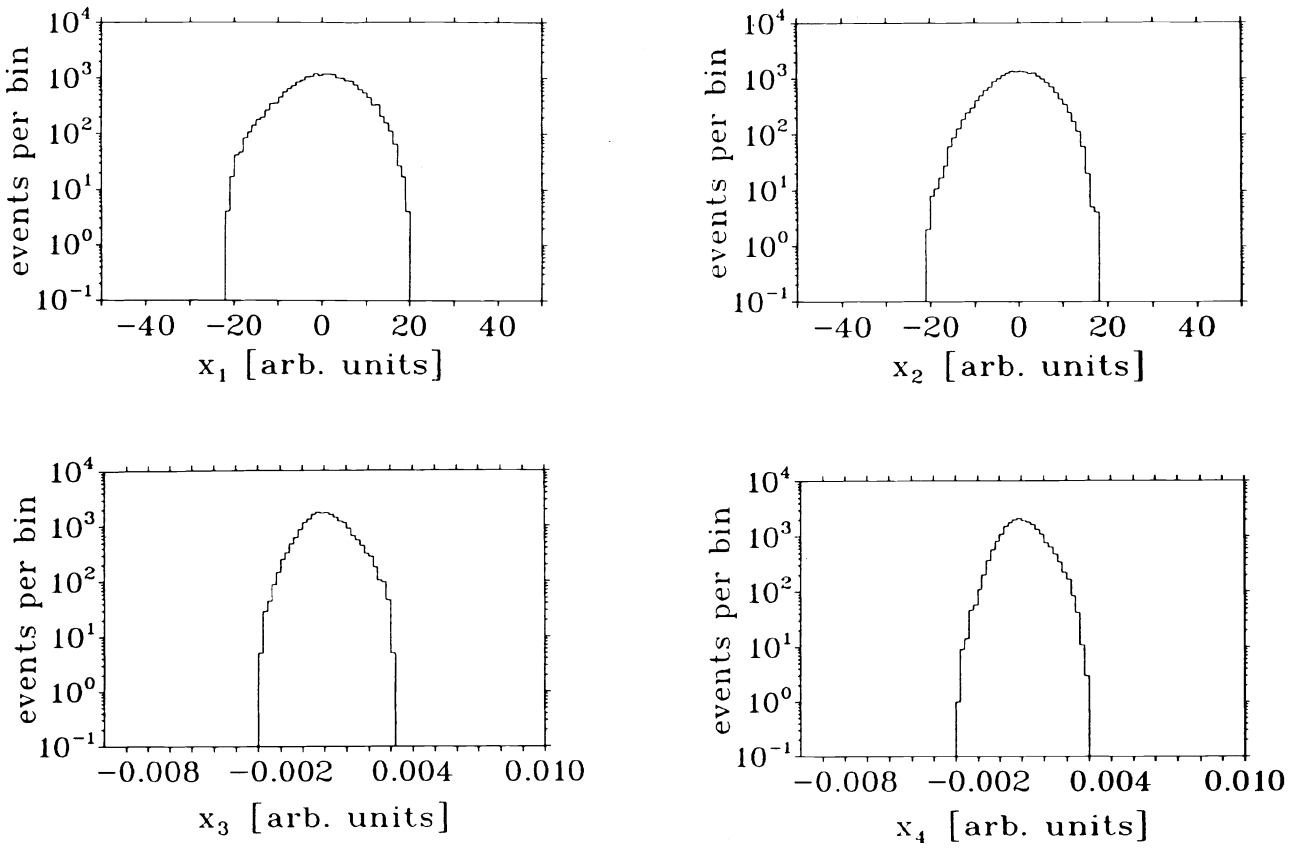

FIG. 7. Distribution of the accepted events vs the parameters x_i (see text).

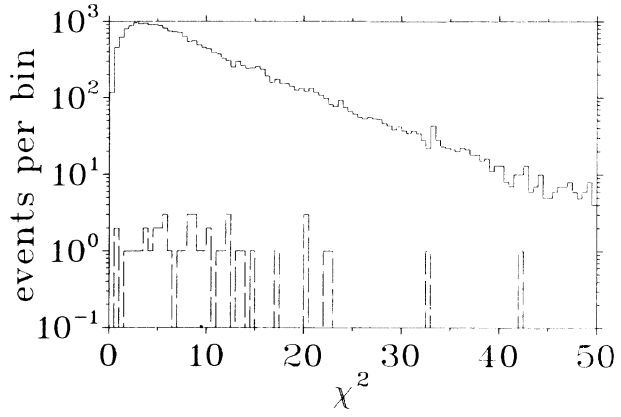

FIG. 8. The χ^2 distribution for the pulse-shape parameters [cf. Eq. (17)] of one run. The solid line represents the events in the main peak; the dashed line those outside the peak. Limiting the allowed χ^2 value for each event to $\chi^2 \leq 10$ (for 7 degrees of freedom) reduces the number of events in the peak by 25% and the number of events outside the peak by 50%.

linewidth of 10.4 keV (FWHM) at an energy of 4120 keV corresponding to the two-body decay of a pion at rest (2) where $m_{\nu_\mu} \leq 270$ keV/c^2 (Ref. 20). There is no evidence for additional lines. The events on the left side of the peak are mainly attributed to muons leaking from the detector Ge2 into the outer annular region of the detector where they produce a signal that is too small to be detected (cf. Sec. III C). This is in agreement with Monte Carlo simulations. The events on the right side of the peak are attributed to muons decaying promptly followed by an accidental coincidence Ge2·($S3+S4$ + Ge3) simulating the decay positron in the event trigger. The cutoff in the muon energy spectrum around 2700 keV ($m_\nu \approx 20$ MeV/c^2) originates from the electronics.[16]

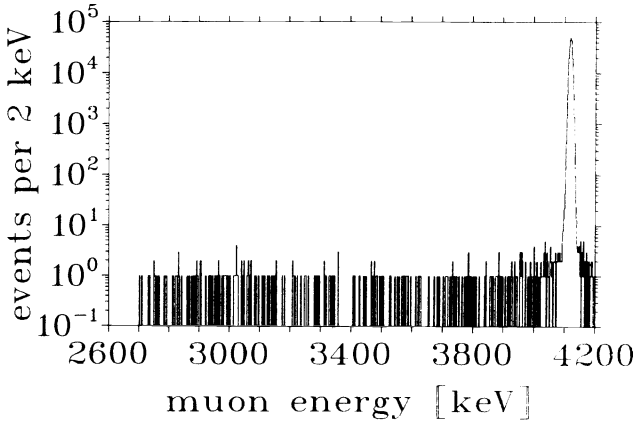

FIG. 9. Spectrum of muon pulse heights as determined from sample points 10 and 4 (for pion decay times from 100 to 200 ns).

B. Determination of the muon line shape

For each run a Gaussian distribution was fitted to the peak of the muon spectrum using the computer program MINUIT (Ref. 19). From the fits the width of the peak was found to be 10.4 keV (FWHM). The χ^2 values of the Gaussian fits to the muon peak for all runs are displayed in Fig. 10. We conclude that the muon energy peak is represented well by a Gaussian distribution.

C. Radiative pion decay

The radiative decay

$$\pi^+ \rightarrow \mu^+ + \nu + \gamma \tag{17}$$

represents a small intrinsic background for this experiment. Castagnoli and Muchnik[21] have studied the radiative decay experimentally. Their results agree well with the theoretical spectrum given by Ioffe and Rudik[22] and by Fialho and Tiomno.[23]

The theoretical energy spectrum given in Ref. 21, convolved with the Gaussian distribution derived from the 4120-keV peak, is displayed in Fig. 11 together with the experimental data. The remaining events after subtraction of this calculated distribution from the experimental data are shown in Fig. 12.

D. Search for additional lines

To obtain upper limits η_i for the branching ratio

$$\Gamma(\pi^+ \rightarrow \mu^+ + \nu_i)/\Gamma(\pi^+ \rightarrow \mu^+ + \nu_\mu)$$

two different methods were used depending on the muon energy. Between 2750 and 4090 keV, i.e., outside the main muon peak, the procedure was as follows.

(a) Energies T_i were selected in steps of 5 keV.

(b) The events in the interval $(T_i - 2\sigma_0)$ to $(T_i + 2\sigma_0)$ were summed to obtain the numbers of events N_i in those peaks; here σ_0 is the rms width of the main muon peak.

(c) From these N_i upper limits, L_i, of numbers of

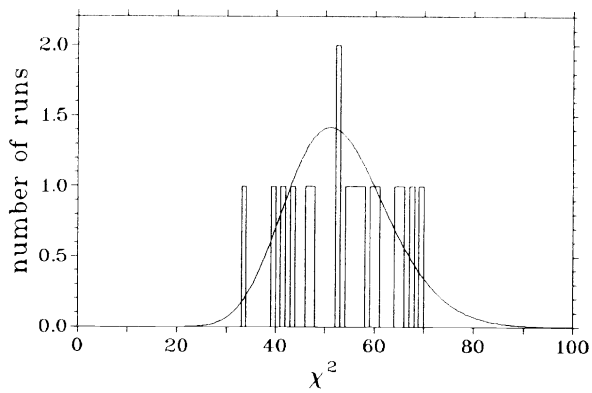

FIG. 10. The χ^2 distribution from the fit of a Gaussian to the main muon peak. The smooth curve represents the expected distribution for the number of degrees of freedom used in the fit (53).

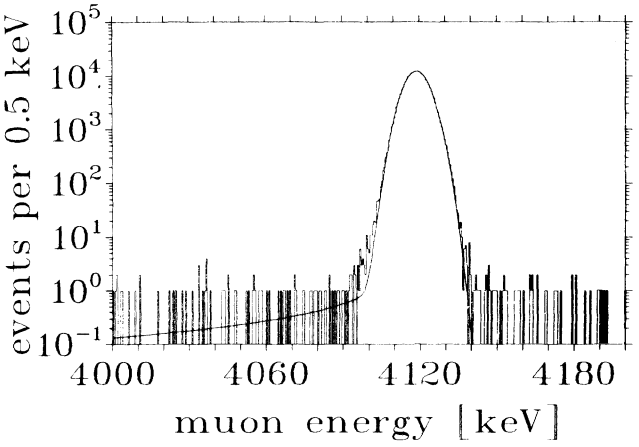

FIG. 11. Gaussian distribution convoluted with the muon energy spectrum from radiative decay and fitted to the experimental data.

events in a hypothetical peak were calculated such that the equation

$$\alpha = \sum_{n=N_i+1}^{\infty} P_{L_i}(n) \tag{18}$$

holds; here $\alpha=0.9$ is the confidence level, N_i is the experimental number of events, and $P_{L_i}(n)$ is the Poisson distribution function with the mean value L_i:

$$P_{L_i}(n)=\frac{L_i^n}{n!}e^{-L_i} . \tag{19}$$

Upper limits η_i for the branching ratio of the pion decay into a muon and a heavy neutrino were obtained by dividing the upper limit L_i of the number of events in a hypothetical line by the number of events N_0 in the main peak.

For neutrino mass values corresponding to muon energies in the region of the main muon peak (4090–4120 keV) the procedure was as follows.

The number of events N_i in a hypothetical line was determined by fitting two Gaussian distributions of the same width to the data, after subtraction of the contribution from the radiative decay. The energy difference between the two peaks, chosen in steps of 5 keV, was fixed. The numbers of events N_0 and N_i, the energy of the main peak T_0, and the common width of the two Gaussians were the free parameters. If the number N_i turned out to be negative, it was replaced by zero, in order to obtain a conservative upper limit. The uncertainty $\Delta N_i(90\%)$ was calculated for a 90% confidence level by the χ^2-minimization program MINUIT (Ref. 19). We used the deviation ΔN_i which corresponds to the maximal extension of the closed hypersurface $\chi^2=\chi_{\min}{}^2 + 1.64$ as the estimate of the uncertainty.

The upper limits η_i in this energy range were determined by adding $\Delta N_i(90\%)$ to the number of events N_i in the hypothetical peak and by dividing this sum by N_0.

In the fits of the two Gaussians to the experimental data the value (χ^2/DF), where DF is the number of degrees of freedom (typically 40), was less than 1.0, except around 4100 keV (cf. Figs. 11 and 12), where the significant positive structure had to be included in the fit. This structure is, however, much narrower than the width expected for an additional peak, and results in values of (χ^2/DF) greater than 1.0, thus leading to χ^2 probabilities of less than 1%. The significantly positive values η_i in this neutrino mass range are therefore not considered as evidence for the existence of a massive neutrino.

A plot of our results is shown in Fig. 13 along with a comparison to earlier experiments.[11,17] Our data yield a considerable improvement in the upper limit η_i of the branching ratio for the decay of a pion into a muon and a heavy neutrino for neutrino masses less than 16 MeV/c^2 and extend the neutrino mass range with significant upper limits down to about 1 MeV/c^2.

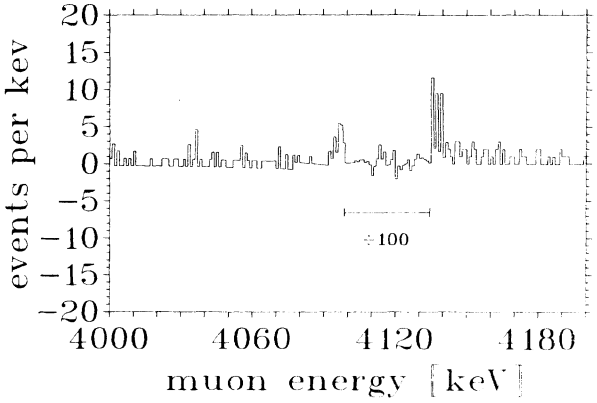

FIG. 12. Experimental data after subtraction of the fit (Fig. 11).

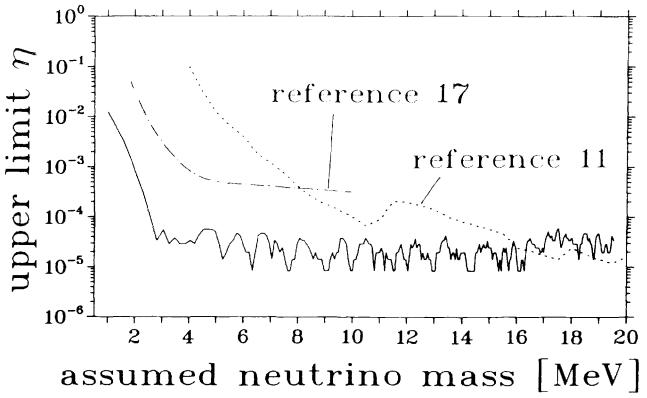

FIG. 13. Upper limit η (90% confidence level) for the decay of a pion into a muon and a massive neutrino as a function of the assumed neutrino mass. Our results are compared with those of Abela *et al.* (Ref. 11) and our previous results (Ref. 17).

ACKNOWLEDGMENTS

We would like to thank Dr. R. Shrock for bringing this problem to our attention. We are indebted to Dr. R. Pehl of Lawrence Berkeley Laboratory for making the Ge detectors. We thank Professor J. P. Blaser of SIN for the hospitality extended to those of us from the University of Virginia. The cooperation of Dr. R. Frosch in the beginning of the experiment is gratefully acknowledged. The experiment would not have been possible without the excellent technical support of many groups at SIN. This work was supported in part by the U.S. Department of Energy, the U.S. National Science Foundation, and the Swiss Institute for Nuclear Research (SIN).

---

*Present address: CERN, CH-1211 Genève, Switzerland.

[1]S. L. Glashow, Nucl. Phys. **22**, 579 (1961); A. Salam, in *Elementary Particle Theory: Relativistic Groups and Analyticity (Nobel Symposium No. 8)*, edited by N. Svartholm (Almqvist and Wiksell, Stockholm, 1968); S. Weinberg, Phys. Rev. Lett. **19**, 1264 (1967).

[2]M. Kobayashi and T. Maskawa, Prog. Theor. Phys. **49**, 652 (1973).

[3]Z. Maki *et al.*, Prog. Theor. Phys. **28**, 870 (1962); B. Pontecorvo, Zh. Eksp. Teor. Fiz. **53**, 1717 (1967) [Sov. Phys. JETP **26**, 984 (1968)].

[4]J. K. Rowley *et al.*, in *Solar Neutrino and Neutrino Astronomy,* Lead, South Dakota, 1984, edited by M. L. Cherry, W. A. Fowler, and K. Lande (AIP Conf. Proc. No. 126) (AIP, New York, 1985).

[5]R. E. Shrock, Phys. Lett. **96B**, 159 (1980).

[6]J. Deutsch, in *Proceedings of the International Europhysics Conference on High Energy Physics,* Bari, Italy, 1985, edited by L. Nitti and G. Preparata (Laterza, Bari, 1985), p. 429ff; F. Vanucci, *ibid.*, p. 1019ff.

[7]H. Albrecht *et al.*, Phys. Lett. **163B**, 404 (1985).

[8]R. Abela *et al.*, SIN Newsletter No. 13, 1980, p. 11.

[9]H. Anderhub *et al.*, SIN Newsletter No. 13, 1980, p. 23.

[10]F. P. Calaprice *et al.*, Phys. Lett. **106B**, 175 (1981).

[11]R. Abela *et al.*, Phys. Lett. **105B**, 263 (1981).

[12]E. V. Shrum and K. O. H. Ziock, Phys. Lett. **37B**, 115 (1971).

[13]SIN Users Handbook, 70 (1981).

[14]B. Jost, Diplomarbeit, Abt. IXB, ETH Zürich, 1981.

[15]R. M. Sternheimer, Phys. Rev. **117**, 485 (1960).

[16]B. Jost, Ph.D. thesis No. 8093, ETH Zürich, 1986.

[17]R. C. Minehart *et al.*, Phys. Rev. Lett. **52**, 804 (1984).

[18]D. C. S. White and W. J. McDonald, Nucl. Instrum. Methods **115**, 1 (1974).

[19]F. James and M. Roos, CERN computer library write up No. D506, 1977.

[20]R. Abela *et al.*, Phys. Lett. **146B**, 431 (1984); B. Jeckelmann *et al.*, Phys. Rev. Lett. **56**, 1444 (1986).

[21]C. Castagnoli and M. Muchnik, Phys. Rev. **112**, 1779 (1958).

[22]B. Ioffe and A. Rudik, Dokl. Akad. Nauk SSSR **82**, 114 (1952).

[23]G. E. A. Fialho and J. Tiomno, An. Bras. Cienc. **24**, 245 (1952).